Systems & Control Transactions

Original Research Article
Peer Reviewed Conference Proceeding
ESCAPE 36 - European Symposium on Computer Aided Process Engineering
Sheffield, UK. 21-24 June 2026

PSE PRESS

Integration of exergy and economic optimization for green hydrogen and power co-generation based on sorbent-enhanced biogas reforming with CO_2 capture

Arthur-Maximilian Báthori[a]*, Calin-Cristian Cormos[a]

[a] Babes-Bolyai University, Faculty of Chemistry and Chemical Engineering, Chemical Engineering Department, 11 Arany Janos, Postal code: 400028, Cluj-Napoca, Romania
* Corresponding Author: arthur.bathori@ubbcluj.ro.

ABSTRACT

In the urgent effort to reduce greenhouse gas (GHG) emissions in the industrial sector, biogas-derived green hydrogen and power co-generation represents a promising solution. Biogas, a renewable and carbon-neutral resource, provides a flexible feedstock for decentralized energy systems, particularly in regions with well-developed agricultural or waste biomass infrastructure. This approach allows the deployment of cost-efficient systems aligned with climate targets and industrial decarbonization roadmaps. Compared to steam methane reforming (SMR), sorbent-enhanced SMR (SE-SMR) with integrated calcium looping (CaL) CO_2 capture reduces process emissions while enhancing hydrogen yield. This study investigates the economic and exergy-based implications of partially splitting hydrogen from a SE-SMR-CaL system producing 50, 000 Nm^3/h of H_2 from desulfurized biogas. Following heat integration using the PINCH methodology, an electrically self-sufficient base case was established. Economic and exergy analyses were conducted in Excel, with cash flow allocation based on exergy contributions. An automated optimization routine identified competitive levelized costs of electricity (LCOE) and hydrogen (LCOH). Results show that increasing the hydrogen split to power generation maintains nearly constant LCOE (<1% variation) while reducing overall exergy efficiency. Partial hydrogen splitting achieves LCOE below 30.5 €/MWh at the expense of increased LCOH, highlighting a trade-off between electricity and hydrogen economics in flexible, multi-vector systems. The workflow demonstrates that incorporating electricity generation into a sorbent-enhanced hydrogen production system using air combustion is technically and economically feasible.

Keywords: Green hydrogen and power, Sorbent-enhanced biogas reforming, Exergy analysis, Modelling, simulation and optimization, Techno-economic assessment

INTRODUCTION

Low carbon technologies and carbon neutrality are key considerations in discussions of a future in which humanity lives in a sustainable manner with respect to available resources. The main challenged addressed in the context of sustainability is anthropogenically induced climate change, which has led to the implementation of a number of significant and ambitious policies worldwide [1]. At the core of these policies is the carbon element, primarily in the form of carbon dioxide (CO_2), a greenhouse gas emitted through various anthropogenic activities, including energy production, the bulk chemical industry, and transportation. By mitigating (or offsetting) CO_2 emissions by choosing renewable raw materials and/or electricity sources, short- to mid-term solutions can be developed that benefit from the use of existing infrastructure [2]. In this context, carbon capture, utilization and storage (CCUS) technologies emerge as carbon sinks by either completely sequestering (via storage) or off-setting (via utilization) the CO_2 footprint of a given technology. However, the transition to carbon-free energy vectors, such as hydrogen and ammonia, represents a long-term solution [3] that requires substantially greater research, development and deployment efforts than previously discussed approaches to increase the

technology readiness level (TRL) and accelerate industrial deployment.

In this context [4], the present work evaluates the techno-economic and exergy-based implications of partially splitting hydrogen (H_2) from a sorbent-enhanced steam methane reforming (SE-SMR) plant, coupled with calcium looping technology (CaL) [5] with a design capacity of 50, 000 Nm3/h of high-purity H_2 for electricity generation. In line with the considerations discussed above, desulfurized biogas is employed as the raw material for hydrogen production [6], offering a sustainable energy pathway for the deployment of an innovative, cost-efficient, and decarbonized system that aligns with climate targets and industrial decarbonization roadmaps. By employing process modelling and simulation using ChemCAD, techno-economic and exergy analyses using Excel, and automation using Visual Basic for Applications (VBA), a robust framework was developed for evaluating multi-product renewable energy systems. In particular, an optimal range for the hydrogen split fraction was identified, within which competitive levelized costs of electricity (LCOH) and hydrogen (LCOH) can be achieved under realistic economic bounds.

PLANT CONFIGURATION, DESIGN ASSUMPTIONS, EXERGY AND ECONOMIC ANALYSIS METHODOLOGY

The plant (Figure 1) is designed to produce 50, 000 Nm^3/h of H_2 using desulfurized biogas, while also providing inherent carbon sequestration through carbonation-calcination cycles. The resulting hydrogen-enriched gas stream from the reformer is further purified via pressure-swing adsorption (PSA). A flexible fraction of pure H_2 is diverted to generate electricity through air combustion for high-pressure (HP) steam generation in a Rankine cycle, while the remainder is compressed and stored for downstream utilization (e.g., chemical applications). The SE-SMR-CaL process employs a dual circulating fluidized bed system, enabling continuous operation with high CO_2 capture efficiency and stable hydrogen production. The process produces high-purity hydrogen and CO_2 streams, with the latter being further processed to meet sequestration or utilization criteria, primarily through water removal using triethylene glycol (TEG) dehydration. In this study, the net power output considers the electricity required for oxygen production from the air separation unit (ASU) and for compressing pure H_2, CO_2, and streams within the TEG unit. After heat integration of the available hot streams using the PINCH methodology to maximize heat recovery (Figure 2), an electrically self-sufficient base case was established.

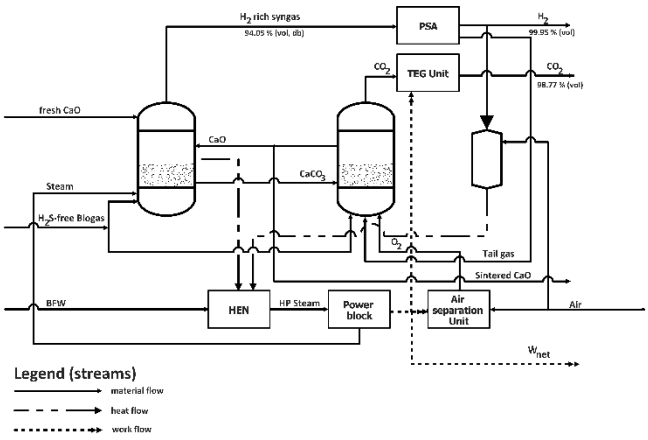

Figure 1. Schematic design of the SE-SMR-CaL plant.

The chemically reactive system within the reformer is described by the following reactions:

r_1 $CH_4 + H_2O \leftrightarrow CO + 3H_2$ ΔH_1 = 206.1 kJ/mol (1)

r_2 $CO + H_2O \leftrightarrow CO_2 + H_2$ ΔH_2 = -41.1 kJ/mol (2)

r_3 $CH_4 + 2H_2O \leftrightarrow CO_2 + 4H_2$ ΔH_3 = 165.0 kJ/mol (3)

r_4 $CaO + CO_2 \leftrightarrow CaCO_3$ ΔH_4 = -178.0 kJ/mol (4)

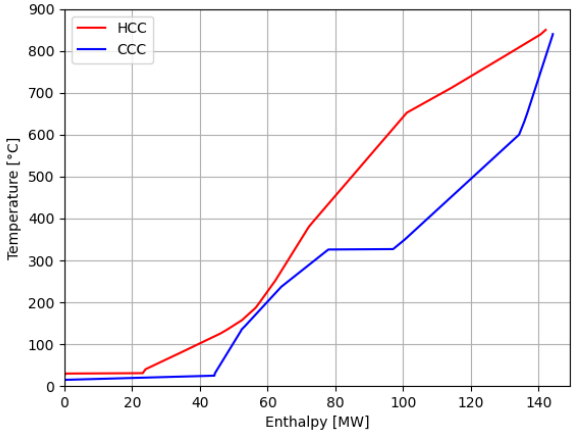

Figure 2. Thermal integration analysis of the SE-SMR-CaL plant.

The reformer was modelled as a kinetic reactor, with the following reaction rates and additional expressions implemented using VBA within ChemCAD [7, 8]:

$$r_1 = \frac{\frac{k_1}{p_{H_2}^{2.5}} \cdot \left(p_{CH_4} \cdot p_{H_2O} - \frac{p_{H_2}^3 \cdot p_{CO}}{K_1}\right)}{\left(1 + K_{CO} \cdot p_{CO} + K_{H_2} \cdot p_{H_2} + K_{CH_4} \cdot p_{CH_4} + \frac{K_{H_2O} \cdot p_{H_2O}}{p_{H_2}}\right)^2} \quad (5)$$

$$r_2 = \frac{\frac{k_2}{p_{H_2}} \cdot \left(p_{CO} \cdot p_{H_2O} - \frac{p_{H_2} \cdot p_{CO_2}}{K_2}\right)}{\left(1 + K_{CO} \cdot p_{CO} + K_{H_2} \cdot p_{H_2} + K_{CH_4} \cdot p_{CH_4} + \frac{K_{H_2O} \cdot p_{H_2O}}{p_{H_2}}\right)^2} \quad (6)$$

$$r_3 = \frac{\frac{k_3}{p_{H_2}^{3.5}} \cdot \left(p_{CH_4} \cdot p_{H_2O}^2 - \frac{p_{H_2}^4 \cdot p_{CO_2}}{K_3}\right)}{\left(1 + K_{CO} \cdot p_{CO} + K_{H_2} \cdot p_{H_2} + K_{CH_4} \cdot p_{CH_4} + \frac{K_{H_2O} \cdot p_{H_2O}}{p_{H_2}}\right)^2} \quad (7)$$

$$r_4 = \frac{3k_4}{\bar{R}_p} \cdot (1 - \bar{X}_{CaO})^{\frac{2}{3}} \cdot \left(\frac{p_{CO_2} - p_{CO_2,eq}}{RT}\right)^{0.66} \quad (8)$$

$$p_{CO_2,eq} = 1.01325 * 10^{\left(\frac{-8308}{T} + 7.079\right)} \quad (9)$$

$$k_i = k_i^0 \cdot e^{-\frac{E_i}{RT}} \quad (10)$$

$$K_j = K_J^0 \cdot e^{-\frac{\Delta H_J}{RT}} \quad (11)$$

The kinetic and thermodynamic parameters employed in expressions (5)-(11) are summarized in Table 1, while general modelling assumptions of the SE-SMR plant are summarized in Table 2.

Table 1: Kinetic and thermodynamic parameters employed for reformer modelling.

Symbol	Value	Unit
k_1^0	4.225•10^{15}	$mol\ bar^{0.5}\ kg^{-1} cat\ s^{-1}$
k_2^0	1.995•10^{6}	$mol\ kg^{-1} cat\ s^{-1}\ bar^{-1}$
k_3^0	1.020•10^{15}	$mol\ kg^{-1} cat\ s^{-1}$
k_4^0	3.05	$m\ s^{-1}$
E_1	240.1	$kJ\ mol^{-1}$
E_2	67.13	$kJ\ mol^{-1}$
E_3	243.9	$kJ\ mol^{-1}$
E_4	32.6	$kJ\ mol^{-1}$
K_C^0	5.8•10^{-4}	$bar^{-0.5}$
K_H^0	1.6•10^{-2}	$bar^{-0.5}$
K_{CO}^0	8.23•10^{-5}	bar^{-1}
$K_{H_2}^0$	6.12•10^{-9}	bar^{-1}
$K_{CH_4}^0$	6.65•10^{-4}	bar^{-1}
$K_{H_2O}^0$	1.77•10^{5}	–
ΔH_C	-42.00	$kJ\ mol^{-1}$
ΔH_H	-16.00	$kJ\ mol^{-1}$
ΔH_{CO}	-70.65	$kJ\ mol^{-1}$
ΔH_{H_2}	-82.90	$kJ\ mol^{-1}$
ΔH_{CH_4}	-32.28	$kJ\ mol^{-1}$
ΔH_{H_2O}	88.68	$kJ\ mol^{-1}$
$\bar{X}_{CaO}$	0.72	–
$\bar{R}_p$	125	μm

Table 2: Primary design assumptions of the SE-SMR-CaL plant.

Plant subsystem	Design specification
Fuel characteristics	Biogas purity (vol. %): 59.75% CH_4, 40.00% CO_2, 0.20% N_2, 0.05% O_2 Lower heating value (LHV): 17.58 MJ/kg
Air Separation Unit (ASU)	Oxygen purity (vol. %): 95% O_2, 3% Ar, 2% N_2 ASU power consumption: 200 kWh/t O_2
Reforming reactor	Reactor temperature & pressure: 650°C & 1.25 bar Reactor model: kinetic reactor Thermal operation mode: isothermal Pressure drop: 0.12 bar Sorbent make-up: 5%
Calcination reactor	Reactor temperature & pressure: 850°C & 1 bar Reactor model: Equilibrium reactor $CaCO_3$ decomposition rate: 98% Pressure drop: 0.15 bar
H_2 purification and compressing	Purification unit: Pressure Swing Adsorption (PSA) H_2 recovery yield: 85% H_2 purity: min. 99.95% (vol.) Final compressing pressure: 60 bar Compressor efficiency: 80%
CO_2 drying and compressing	Drying unit: TEG (Triethylene glycol) CO_2 composition (vol. %): >95% CO_2, <2, 000 ppm CO, <250 ppm H_2O, <100 ppm H_2S, <4% non-condensable gases (N_2, H_2, Ar) Delivery pressure: 120 bar
Steam cycle	HP steam parameters: 600°C & 120 bar LP steam parameters: 152°C & 1.25 bar Condensation pressure (steam turbine): 0.05 bar Steam expander efficiency: 92%
Heat exchanger network (HEN)	ΔT_{min}: 10°C Pressure drop: 2 - 4% of inlet pressure
Thermodynamic packages	Biogas processing unit: SRK Gas compression units: BWRS CO_2 drying unit: TEG Dehydration

Exergy efficiencies (ε) are defined according to the fuel (F)-product (P) paradigm [9], accounting for the physical and chemical contributions of inlet and outlet streams within a given control volume, defined such that the boundary temperature equals the environmental temperature. In this study, pre-treated biogas, oxygen from the ASU, required boiler feed water (BFW) for steam reforming, and fresh CaO are considered fuels, while the purified H_2, captured and processed CO_2, and net electricity output are treated as products. Exergy losses are attributed to CO_2 emissions from the TEG unit, removed sintered sorbent stream, and process water discharged as condensate streams.

$$\varepsilon = \frac{\dot{E}_P}{\dot{E}_F} = 1 - \frac{\dot{E}_D + \dot{E}_L}{\dot{E}_F} \quad (12)$$

$$e^{PH} = (h - h_0) - T_0 * (s - s_0) \quad (13)$$

$$\overline{e}^{CH} = \sum_1^k x_k * \overline{e}_k^{CH} + \overline{R}T_0 * \sum_1^k x_k * ln\,(x_k) \quad (14)$$

$$\dot{E} = \dot{m} * \left(e^{PH} + e^{CH}\right) \quad (15)$$

To facilitate the computation of chemical exergy using ChemCAD's thermodynamic packages, a custom unit operation was developed to duplicate a stream with a specified composition at a given temperature and pressure and bring it to the restricted dead state (RDS) by flashing it at T_0 = 25 °C and p_0 = 1 bar. All RDS streams are subsequently mixed to verify the mass balance of the overall plant.

The economic analysis focuses around the estimation of the following relevant economic performance indicators:

Capital expenditure of a process unit (C_E) with capacity Q is calculated using the cost correlation approach [10], which considers base cost of the evaluated subsystem (C_B), its corresponding base production size (Q_B) and a technological maturity exponent (M):

$$C_E = C_B * \left(\frac{Q}{Q_B}\right)^M \quad (16)$$

The reference data (C_B, Q_B and M) were extracted from the literature and the outdated values were updated to the present-day conditions by usage of Chemical Engineering Plant Cost Index (CEPCI):

$$\frac{Cost_{y1}}{Cost_{y2}} = \frac{CEPCI_{y1}}{CEPCI_{y2}} \quad (17)$$

Operational and maintenance (O&M) costs account for both fixed costs (e.g., maintenance, labour, and administrative expenses) and variable costs (e.g., feedstock chemicals, catalyst replacement, cold utilities, and costs associated with CO_2 transport and storage) over the operational lifetime of the plant.

The levelized cost of hydrogen (LCOH) was calculated as the sum of the annualized capital cost ($CC_{Annualized}$), assuming straight-line depreciation, and the operational and maintenance (O&M) costs, divided by the annual hydrogen thermal output ($Q_{H2, Annual}$):

$$LCOH = \frac{CC_{Annualized} + O\&M}{Q_{H_{2,Annual}}} \quad (17)$$

The Levelized cost of electricity (LCOE) was computed in a similar manner than levelized cost of hydrogen (LCOH), with additional consideration for the correlation factors that account for the combined energy output (hydrogen and net power) of the plant.

Varying the hydrogen split fraction decreases the required capacity for the hydrogen compression system while increasing the power block capacity, impacting capital expenditures and, consequently, levelized costs. The optimization focuses on determining the net present value (NPV) of the overall plant, accounting for changes in the cost correlation method and allocating the cash flow factor based on the exergy values of the produced hydrogen and electricity.

Excel Solver is used to determine the levelized costs of electricity (LCOE) and hydrogen (LCOH) that yield an NPV of zero, subject to non-negativity constraints:

Find LCOE, LCOH such that: NPV(LCOE, LCOH) = 0, subject to LCOE ≥ 0, LCOH ≥ 0, NPV ≥ 0.

Automation is achieved by employing the sensitivity study tool and data maps within ChemCAD to extract the relevant thermodynamic data of the main material streams (specific enthalpy, specific entropy, stream composition, stream mass rate) and unit operation parameters (e.g., compressor power, divider split fraction), in combination with a VBA subroutine that links each sensitivity study run to an instance of Excel Solver:

```
Sub RunExcelSolverFromChemCAD()
 Dim xlApp As Object
 Dim xlWB As Object
 Set xlApp = CreateObject("Excel.Application")
 xlApp.Visible = False
 Set xlWB = xlApp.Workbooks.Open("path_to_solver")
 xlApp.RUN "RunSolverAuto"
 xlWB.Close SaveChanges:=True
 xlApp.Quit
 Set xlWB = Nothing
 Set xlApp = Nothing
End Sub
```

RESULTS AND DISCUSSION

The mathematical model of the plant was validated primarily by analyzing the dry volumetric composition of the simulated reformer gaseous output with respect to available experimental data [12, 13] (Table 3).

Table 3: Validation of the kinetic reformer model.

Parameter	Simulation	Experimental
% CH_4	2.15	2-2.5
% CO + CO_2 + N_2	3.8	3-4
% H_2	94.05	94-94.5
CH_4 conversion	90.77	90

As shown, the simulation data are in range and close agreement to the experimental data, with relative errors for hydrogen composition and methane conversion below 0.5%. This underlines the reliability of the model and the robust behaviour of the kinetically modelled reformer. A more detailed model validation is presented in a previous work of the authors [11] which serves as the basis of the current optimization study, including sorbent deactivation [14] as a function of the number of looping cycles and several arguments for the sorbent make-up fraction and selected mean sorbent conversion within the reformer.

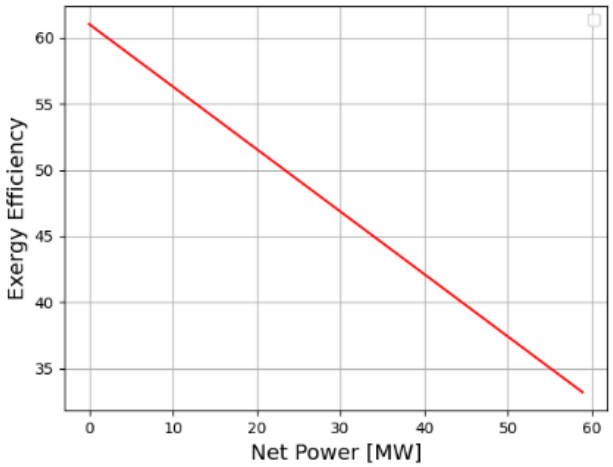

Figure 3. Plant exergy efficiency variation with hydrogen split fraction.

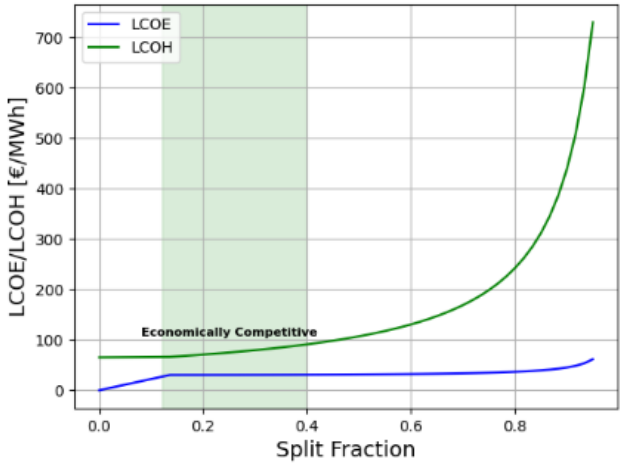

Figure 4. LCOE and LCOH dependence of hydrogen split fraction in the first sensitivity analysis.

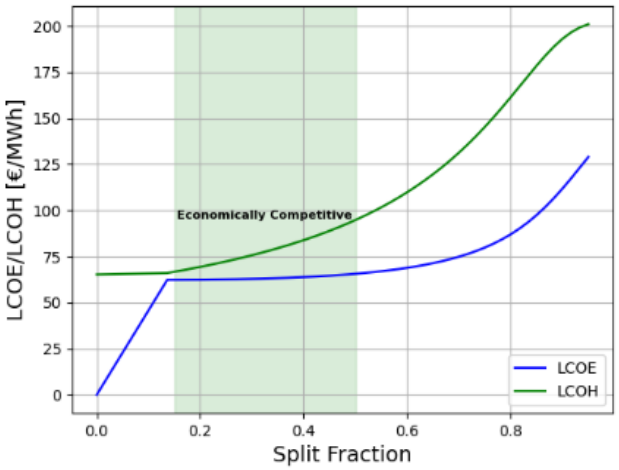

Figure 5. LCOE and LCOH dependence of hydrogen split fraction in the second sensitivity analysis.

Once the steady-state output of the reformer was validated, two successive sensitivity analyses were conducted in ChemCAD, employing the previously mentioned data map and Excel solver configuration. Both runs indicated that as the hydrogen split fraction for electricity generation increases up to about 0.40, the levelized cost of electricity (LCOE) remains essentially constant, varying by less than 1%, while the overall system exergy efficiency declines. This highlights an important compromise between electricity generation and exergy efficiency. The observed linear decrease in exergy efficiency (Figure 3) is expected, as the high chemical exergy of the pure hydrogen stream is inefficiently utilized to generate steam and, subsequently, electricity through combustion, an inherent exergy sink, and a Rankine cycle, operating at constant efficiency across all split fractions.

The optimization results reveal two distinct operational regimes. In the first case (Figure 4), a plateau in electricity cost is observed where LCOE remains below 30.5 €/MWh, while the LCOH steadily increases from 80 to 100 €/MWh in a linear manner. Beyond this split-fraction range, the LCOH rises exponentially up to 700 €/MWh, highlighting a threshold where hydrogen production becomes economically prohibitive. In this regime, the economic burden is primarily borne by hydrogen production, as electricity costs remain stable up to a split fraction of 0.85.

In the second optimization study (Figure 5), the solver was initialized to previously obtained values [11], with both LCOE and LCOH starting around 60-70 €/MWh. In this case, LCOE remains approximately constant across a wider range of hydrogen split fractions (up to about 0.55), while LCOH increases gradually to 100 €/MWh and, at high split fractions, only reaches about 200 €/MWh. These findings indicate that while affordable electricity prices can be maintained across a broad operational range, hydrogen costs are highly

sensitive to the split fraction beyond certain thresholds. In essence, the system preserves economically competitive electricity prices across a wide operating range by progressively transferring the cost burden to hydrogen production as the split fraction increases.

The results further indicate an important trade-off between electricity and hydrogen economics. Allowing for a moderate increase in electricity costs (approximately 50% compared to the first operational regime) enables hydrogen production costs to remain stable over a wider range of hydrogen split fractions. This defines a flexible operating window, extending up to a split fraction of 0.55, within which the plant can simultaneously supply moderately priced electricity and economically competitive hydrogen. The application of exergy-based allocation to the cash flow factor enhances the interpretation of these results by revealing the relative efficiency and economic contribution of each product, thereby supporting more robust design and investment decisions for integrated multi-vector energy systems.

From a global market perspective, the LCOE achieved in the most competitive scenarios (< 30.5 €/MWh) is below typical world averages for newly commissioned renewable generation such as solar PV (about 40–60 €/MWh [15]) and onshore wind (about 42 €/MWh [16]). Even the higher-cost case (about 60–70 €/MWh) remain within the range of real-world LCOE values, indicating that the proposed system is economically feasible and competitive in multiple energy markets.

CONCLUSIONS

This study shows that partial hydrogen splitting can be optimized to balance electricity affordability and hydrogen production costs, highlighting a clear trade-off between electricity and hydrogen economics. Two distinct operational cases were identified, showing that low-cost electricity can be maintained across a range of split fractions while hydrogen costs remain economically competitive. As a key finding, despite the overall variability in LCOH, operating at a hydrogen split fraction between 0.4 and 0.5 provides a reliable and economically competitive range for hydrogen production.

The proposed methodology provides a reproducible and adaptable framework for evaluating multi-product renewable energy systems, which can be extended to alternative hydrogen-to-power pathways, including fuel cells, supporting the development of sustainable and flexible hybrid energy strategies.

ACKNOWLEDGEMENTS

This work was supported by a grant of the Ministry of Education and Research, CCCDI – UEFISCDI, project number: PN-IV-P8-8.1-PRE-HE-ORG-2024-0228, within PNCDI IV.

REFERENCES

1. United Nations Framework Convention on Climate Change. Paris agreement. https://unfccc.int/sites/default/files/english_paris_agreement.pdf
2. Davoodi S, Al-Shargabi M, Wood DA, Rukavishnikov VS, Minaev KM. Review of technological progress in carbon dioxide capture, storage, and utilization. Gas Science and Engineering 117:205070 (2023). https://doi.org/10.1016/j.jgsce.2023.205070
3. Flores F, Feijoo F, DeStephano P, Herc L, Pfeifer A, Dui? N. Assessment of the impacts of renewable energy variability in long-term decarbonization strategies. Applied Energy 368:123464 (2024). https://doi.org/10.1016/j.apenergy.2024.123464
4. Masoudi Soltani S, Lahiri A, Bahzad H, Clough P, Gorbounov M, Yan Y. Sorption-enhanced steam methane reforming for combined CO2 capture and hydrogen production: a state-of-the-art review. Carbon Capture Science & Technology 1:100003 (2021). https://doi.org/10.1016/j.ccst.2021.100003
5. Arias B, Alvarez Criado Y, Méndez A, Marqués P, Finca I, Abanades JC. Pilot testing of calcium looping at TRL7 with co₂ capture efficiencies toward 99%. Energy Fuels 38:14757-14764 (2024). https://doi.org/10.1021/acs.energyfuels.4c02472
6. Fagerström Anton, Al Seadi Teodorita, Rasi Saija, Briseid Tormod. The role of anaerobic digestion and biogas in the circular economy. IEA Bioenergy 2019.
7. Xu J, Froment GF. Methane steam reforming, methanation and water?gas shift: I. intrinsic kinetics. AIChE Journal 35:88-96 (2004). https://doi.org/10.1002/aic.690350109
8. Johnsen K, Grace JR, Elnashaie SSEH, Kolbeinsen L, Eriksen D. Modeling of sorption-enhanced steam reforming in a dual fluidized bubbling bed reactor. Ind. Eng. Chem. Res. 45:4133-4144 (2006). https://doi.org/10.1021/ie0511736
9. Bejan A, Tsatsaronis G, Moran M. Thermal design and optimization. first edition, John Wiley & Sons Hoboken, USA (1995)
10. Smith R. Chemical process design and integration. second edition, Wiley, Hoboken, USA (2016)
11. Báthori AM, Cormos CC. Green hydrogen production by intensified biogas reforming via sorption-enhanced technology: an energy, exergy, economic and environmental (4E) analysis. International Journal of Hydrogen Energy 155:150363 (2025).

https://doi.org/10.1016/j.ijhydene.2025.150363
12. Hyper - Bulk hydrogen production by sorbent enhanced steam reforming. https://hyperh2.co.uk/
13. García-Lario AL, Aznar M, Martinez I, Grasa GS, Murillo R. Experimental study of the application of a nio/nial2o4 catalyst and a cao-based synthetic sorbent on the sorption enhanced reforming process. International Journal of Hydrogen Energy 40:219-232 (2015). https://doi.org/10.1016/j.ijhydene.2014.10.033
14. Greco-Coppi M, Strohle J, Epple B. A carbonator model for CO_2 capture based on results from pilot tests. Part II: deactivation and reaction model. *Chem Eng J* 508:159041 (2025) https://doi.org/10.1016/j.apenergy.2016.12.153
15. Lai CS, McCulloch MD. Levelized cost of electricity for solar photovoltaic and electrical energy storage. Applied Energy 190:191-203 (2017). https://doi.org/10.1016/j.apenergy.2016.12.153
16. Stehly T, Duffy P, Hernando DM, Cost of Wind Energy Review: 2024 Edition. National Renewable Energy Laboratory 2024